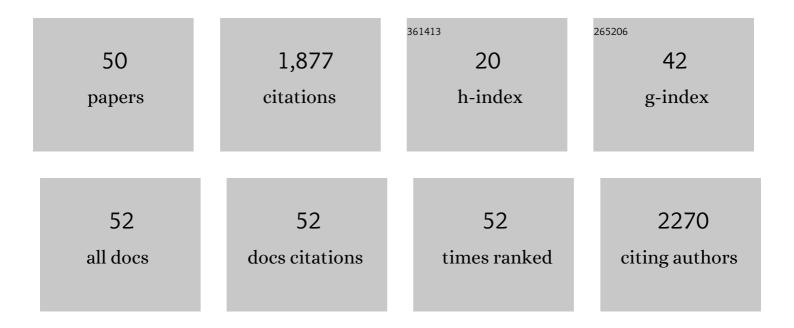
Sophie Zinn-Justin

List of Publications by Year in descending order

Source: https://exaly.com/author-pdf/6070956/publications.pdf Version: 2024-02-01



#	Article	IF	CITATIONS
1	Dissecting the roles of Haspin and VRK1 in histone H3 phosphorylation during mitosis. Scientific Reports, 2022, 12, .	3.3	8
2	Protein structural and mechanistic basis of progeroid laminopathies. FEBS Journal, 2021, 288, 2757-2772.	4.7	23
3	The phospho-dependent role of BRCA2 on the maintenance of chromosome integrity. Cell Cycle, 2021, 20, 731-741.	2.6	3
4	Di-phosphorylated BAF shows altered structural dynamics and binding to DNA, but interacts with its nuclear envelope partners. Nucleic Acids Research, 2021, 49, 3841-3855.	14.5	25
5	Intrinsic Disorder and Phosphorylation in BRCA2 Facilitate Tight Regulation of Multiple Conserved Binding Events. Biomolecules, 2021, 11, 1060.	4.0	6
6	BRCA2 binding through a cryptic repeated motif to HSF2BP oligomers does not impact meiotic recombination. Nature Communications, 2021, 12, 4605.	12.8	8
7	Lamin B1 sequesters 53BP1 to control its recruitment to DNA damage. Science Advances, 2021, 7, .	10.3	21
8	1H, 13C and 15N backbone resonance assignment of the human BRCA2 N-terminal region. Biomolecular NMR Assignments, 2020, 14, 79-85.	0.8	6
9	Cyclic imine toxins survey in coastal european shellfish samples: Bioaccumulation and mode of action of 28-O-palmitoyl ester of pinnatoxin-G. first report of portimine-A bioaccumulation Harmful Algae, 2020, 98, 101887.	4.8	18
10	Architecture of the flexible tail tube of bacteriophage SPP1. Nature Communications, 2020, 11, 5759.	12.8	37
11	Sensitivityâ€Enhanced 13 Câ€NMR Spectroscopy for Monitoring Multisite Phosphorylation at Physiological Temperature and pH. Angewandte Chemie, 2020, 132, 10497-10501.	2.0	6
12	Sensitivityâ€Enhanced ¹³ Câ€NMR Spectroscopy for Monitoring Multisite Phosphorylation at Physiological Temperature and pH. Angewandte Chemie - International Edition, 2020, 59, 10411-10415.	13.8	15
13	The high protein expression of FOXO3, but not that of FOXO1, is associated with markers of good prognosis. Scientific Reports, 2020, 10, 6920.	3.3	5
14	Proper chromosome alignment depends on BRCA2 phosphorylation by PLK1. Nature Communications, 2020, 11, 1819.	12.8	38
15	An Emerin LEM-Domain Mutation Impairs Cell Response to Mechanical Stress. Cells, 2019, 8, 570.	4.1	14
16	Combining Homologous Recombination and Phosphopeptide-binding Data to Predict the Impact of <i>BRCA1</i> BRCT Variants on Cancer Risk. Molecular Cancer Research, 2019, 17, 54-69.	3.4	21
17	1H, 13C and 15N backbone resonance assignment of the lamin C-terminal region specific to prelamin A. Biomolecular NMR Assignments, 2018, 12, 225-229.	0.8	1
18	Proteinâ^'Protein Interfaces Probed by Methyl Labeling and Protonâ€Detected Solidâ€State NMR Spectroscopy. ChemPhysChem, 2018, 19, 2457-2460.	2.1	15

SOPHIE ZINN-JUSTIN

#	Article	IF	CITATIONS
19	Structural analysis of the ternary complex between lamin A/C, BAF and emerin identifies an interface disrupted in autosomal recessive progeroid diseases. Nucleic Acids Research, 2018, 46, 10460-10473.	14.5	54
20	Structures of biomolecular complexes by combination of NMR and cryoEM methods. Current Opinion in Structural Biology, 2017, 43, 104-113.	5.7	32
21	High affinity anchoring of the decoration protein pb10 onto the bacteriophage T5 capsid. Scientific Reports, 2017, 7, 41662.	3.3	21
22	Bacteriophage Tailâ€Tube Assembly Studied by Protonâ€Detected 4D Solidâ€State NMR. Angewandte Chemie - International Edition, 2017, 56, 9497-9501.	13.8	27
23	Emerin selfâ€assembly mechanism: role of the LEM domain. FEBS Journal, 2017, 284, 338-352.	4.7	16
24	Bacteriophage Tailâ€Tube Assembly Studied by Protonâ€Detected 4D Solidâ€State NMR. Angewandte Chemie, 2017, 129, 9625-9629.	2.0	6
25	Purification and Structural Analysis of LEM-Domain Proteins. Methods in Enzymology, 2016, 569, 43-61.	1.0	7
26	1H, 13C and 15N backbone resonance assignment of the intrinsically disordered region of the nuclear envelope protein emerin. Biomolecular NMR Assignments, 2016, 10, 179-182.	0.8	8
27	Bacteriophage SPP1 Tail Tube Protein Self-assembles into β-Structure-rich Tubes. Journal of Biological Chemistry, 2015, 290, 3836-3849.	3.4	24
28	Structural rearrangements in the phage head-to-tail interface during assembly and infection. Proceedings of the National Academy of Sciences of the United States of America, 2015, 112, 7009-7014.	7.1	53
29	Muscular Dystrophy Mutations Impair the Nuclear Envelope Emerin Self-assembly Properties. ACS Chemical Biology, 2015, 10, 2733-2742.	3.4	16
30	Automated classification of tailed bacteriophages according to their neck organization. BMC Genomics, 2014, 15, 1027.	2.8	203
31	Inhibition of TGF-β Signaling at the Nuclear Envelope: Characterization of Interactions Between MAN1, Smad2 and Smad3, and PPM1A. Science Signaling, 2013, 6, ra49.	3.6	44
32	Solution structure of gp17 from the <i>Siphoviridae</i> bacteriophage SPP1: Insights into its role in virion assembly. Proteins: Structure, Function and Bioinformatics, 2012, 80, 319-326.	2.6	15
33	Structural Analysis of the Smad2â^MAN1 Interaction That Regulates Transforming Growth Factor-β Signaling at the Inner Nuclear Membrane. Biochemistry, 2010, 49, 8020-8032.	2.5	29
34	Structure of bacteriophage SPP1 head-to-tail connection reveals mechanism for viral DNA gating. Proceedings of the National Academy of Sciences of the United States of America, 2009, 106, 8507-8512.	7.1	107
35	The checkpoint Saccharomyces cerevisiae Rad9 protein contains a tandem tudor domain that recognizes DNA. Nucleic Acids Research, 2007, 35, 5898-5912.	14.5	26
36	Solution structure of the region 51–160 of human KIN17 reveals an atypical winged helix domain. Protein Science, 2007, 16, 2750-2755.	7.6	20

SOPHIE ZINN-JUSTIN

#	Article	IF	CITATIONS
37	A Tandem of SH3-like Domains Participates in RNA Binding in KIN17, a Human Protein Activated in Response to Genotoxics. Journal of Molecular Biology, 2006, 364, 764-776.	4.2	20
38	Crystallization and halide phasing of the C-terminal domain of human KIN17. Acta Crystallographica Section F: Structural Biology Communications, 2006, 62, 245-248.	0.7	7
39	NMR Assignment of Region 51–160 of Human KIN17, a DNA and RNA-binding Protein. Journal of Biomolecular NMR, 2006, 36, 29-29.	2.8	3
40	The Carboxyl-terminal Nucleoplasmic Region of MAN1 Exhibits a DNA Binding Winged Helix Domain. Journal of Biological Chemistry, 2006, 281, 18208-18215.	3.4	60
41	Compound heterozygosity for mutations in LMNA causes a progeria syndrome without prelamin A accumulation. Human Molecular Genetics, 2006, 15, 2509-2522.	2.9	83
42	Boundaries and physical characterization of a new domain shared between mammalian 53BP1 and yeast Rad9 checkpoint proteins. Protein Science, 2005, 14, 1827-1839.	7.6	13
43	The Tudor Tandem of 53BP1. Structure, 2004, 12, 1551-1562.	3.3	96
44	Letter to the Editor:1H,13C and15N Resonance Assignments of the Region 1463-1617 of the Mouse p53 Binding Protein 1 (53BP1). Journal of Biomolecular NMR, 2004, 28, 303-304.	2.8	4
45	The Carboxyl-Terminal Region Common to Lamins A and C Contains a DNA Binding Domainâ€. Biochemistry, 2003, 42, 4819-4828.	2.5	157
46	The Ig-like Structure of the C-Terminal Domain of Lamin A/C, Mutated in Muscular Dystrophies, Cardiomyopathy, and Partial Lipodystrophy. Structure, 2002, 10, 811-823.	3.3	252
47	1H, 13C and 15N resonance assignments of the C-terminal domain of human lamin A/C. Journal of Biomolecular NMR, 2002, 22, 371-372.	2.8	4
48	Structural analysis of emerin, an inner nuclear membrane protein mutated in X-linked Emery-Dreifuss muscular dystrophy. FEBS Letters, 2001, 501, 171-176.	2.8	62
49	Variability in automated assignment of NOESY spectra and three-dimensional structure determination: a test case on three small disulfide-bonded proteins. Journal of Biomolecular NMR, 2001, 19, 49-62.	2.8	24
50	Structural Characterization of the LEM Motif Common to Three Human Inner Nuclear Membrane Proteins. Structure, 2001, 9, 503-511.	3.3	107